

Model of radiative transfer in fibrous media— matrix method

P. BOULET, G. JEANDEL and G. MORLOT

Laboratoire Infrarouge, L.M.C.P.I.—U.R.A. 809, Faculté des Sciences BP239,
54506 Vandoeuvre-Les-Nancy Cedex, France

(Received 7 December 1992 and in final form 25 June 1993)

Abstract—A matrix model of radiative transfer is presented. Beginning with the radiative properties of a medium, two characteristic matrices representing the transmissive and reflective contributions to energy transfer are written and the intensity distribution is then calculated numerically. Applications to pure radiative transfer and combined transfer with conduction are presented. A case of a material composed of silica fibres is discussed, showing that the model is in good agreement with experimental results. Since no simplifying hypotheses concerning the properties of the medium are incorporated into the model, it can be used to study any fibrous medium.

1. INTRODUCTION

RADIATIVE transfer through fibrous media is the subject of a large number of studies because of its multiple practical applications, especially in thermal insulation. A theoretically derived model for the characterization of radiative transfer will be presented in the current work, one which can be easily applied to the explanation of experimental measurements.

The basics of our problem are found in works on radiative transfer in participating media. Several books are available that treat the modelling aspect, including that by Ozisik [1] on the different existing methods of solution and another by Chandrasekhar [2] which is more particularly concerned with the discrete ordinates methods. In the field of approximate methods the two-flux approximation is commonly used, namely by Tong and Tien [3, 4], or in recent works by Guilbert [5, 6], Banner [7] and Jeandel *et al.* [8]. The results obtained are interesting, but a more thorough modelling treatment was needed in order to obtain a better description. Roux *et al.* [9], and more recently Houston [10], addressed this point by using a numerical treatment based on the discrete ordinates method. In a different domain, but still using such spatial discretization methods as the starting point, matrix-methods are used for the study of radiative transfer in gases. Goody and Yung [11], Flatau and Stephens [12], Waterman [13] and Wiscombe [14] have all written good reviews on this subject.

We focused our attention on the calculation of precise values of the radiative properties, taking into account their spectral and directional variations. The interaction between a fibre and radiation is the basis of the model presented here. Some solution methods, such as those of Kerker [15] and Lind and Greenberg [16] can be directly written into numerical form. The case of a medium composed of fibres may then be

studied based on the work of Lee [17, 18], who showed the influence of the morphological characteristics of the medium, and in particular the orientation of the fibres, on the radiative transfer.

Considering the results obtained, it becomes possible to develop a formulation that is physically representative of the observed scattering phenomena. Furthermore, an understanding of the strongly anisotropic nature of this sort of problem allows one to perform an appropriate discretization of the problem and thus properly use matrix methods [19].

We will first examine how to determine the usual radiative properties: the spectral absorption, scattering and extinction coefficients. We will also define parameters called 'bidirectional scattering coefficients', which offer a convenient representation of the scattering geometry. The adaptation of the radiative transfer equation to matrix form, and its subsequent solution will then be discussed. Following this, two different physical cases can be treated with the model developed here, the first being purely radiative as it appears in transmission or reflexion measurements, and the second being radiation combined with conduction as encountered in the simulation of heat transfer through fibrous insulating materials.

Model simulations on a medium composed of silica fibres will be compared to results obtained from experiments in the case of fibres oriented in planes parallel to the boundaries.

2. MODEL DEVELOPMENT

Consider the problem of radiation heat transfer through a planar fibrous medium. The associated transfer equation represents the wave-matter interactions, taking into account the medium properties. For an absorbing-scattering-emitting medium, as-

NOMENCLATURE

J_λ	source function	λ_c	thermal conductivity
L	medium thickness	μ	$\cos \xi$
L_λ	spectral intensity	ξ	polar angle
$L_{0\lambda}$	black body spectral intensity	$\sigma_{a\lambda}$	spectral absorption coefficient
N	density of fibre	$\sigma_{s\lambda}$	spectral scattering coefficient
P_λ	spectral phase function	$\sigma_{e\lambda}$	spectral extinction coefficient
Q_λ	monochromatic efficiency	ω	azimuthal angle.
Q_c	heat flux by conduction		
Q_r	heat flux by radiation		
r	radius of fibre		
T	temperature		
y	abscissa.		
Greek symbols		Subscripts	
λ	wavelength	a	absorption
		e	extinction
		f	fibre
		s	scattering.

suming transfer in the y -direction with axial symmetry, this equation can be written :

$$\mu \frac{\partial L_\lambda(y, \mu)}{\partial y} = -\sigma_{e\lambda}(\mu)L_\lambda(y, \mu) + J_\lambda(y, \mu) \quad (1)$$

where μ is the cosine of the polar angle between the directions of propagation and transfer.

In equation (1) J_λ is generally called the source-function, which represents internal emission and the intensity of the scattering in the μ -direction :

$$J_\lambda(y, \mu) = \frac{1}{2} \int_{\mu_s = -1}^1 \sigma_{s\lambda} P_\lambda(\mu_s \rightarrow \mu) L_\lambda(y, \mu_s) d\mu_s + \sigma_{a\lambda}(\mu) L_{0\lambda}[T(y)] \quad (1')$$

where $L_{0\lambda}(T)$ is the monochromatic intensity of the black body at temperature T .

The calculation of the different radiative properties used here is essential. As can be seen from the above expressions, these are both spectral and directional variables. Moreover, in this general form of the radiative transfer equation, the phase function does not appear alone, but rather in a product with the scattering coefficient. These problems will be discussed in Section 3.

Equation (1) poses a problem linked with the integral term. Dividing the problem space into a given number of directions yields the following system of differential equations :

$$\mu_i \frac{\partial L_\lambda(y, \mu_i)}{\partial y} = -\sigma_{e\lambda}(\mu_i) L_\lambda(y, \mu_i) + \sigma_{a\lambda}(\mu_i) L_{0\lambda}[T(y)] + \sum_{j=1}^m C_{ij} L_\lambda(y, \mu_j) \quad (2)$$

$$\text{for } i = 1, \dots, m$$

where the monochromatic coefficients C_{ij} take into account the scattering representation and the weights of integration.

Using the spatial discretization shown schematically in Fig. 1, equation (2) can be rewritten in matrix form. Let us define four column vectors of m elements : $L_\lambda^+(y)$, $L_\lambda^-(y)$, $B_\lambda^+(y)$ and $B_\lambda^-(y)$ such that :

for $i = 1, \dots, (m/2)$:

$$L_\lambda^+(y) = [L_\lambda(y, \mu_i)]$$

and

$$L_\lambda^-(y) = [L_\lambda(y, \mu_{-i})]$$

where $-\mu_i = \mu_{-i}$;

$$B_\lambda^+(y) = \left[\begin{array}{c} \sigma_{a\lambda}(\mu_i) \\ \mu_i \end{array} L_{0\lambda}[T(y)] \right]$$

and

$$B_\lambda^-(y) = \left[\begin{array}{c} \sigma_{a\lambda}(\mu_{-i}) \\ \mu_{-i} \end{array} L_{0\lambda}[T(y)] \right].$$

The symmetry properties obtained with this representation allow us to write the radiative transfer equation as (see Flatau and Stephens [12] and Stamnes and Swanson [20]) :

$$\left[\frac{\partial L_\lambda(y)}{\partial y} \right] = [A_\lambda][L_\lambda(y)] + [B_\lambda(y)] \quad (3)$$

where

$$[L_\lambda(y)] = \left[\begin{array}{c} L_\lambda^+(y) \\ L_\lambda^-(y) \end{array} \right]$$

and

$$[B_\lambda(y)] = \left[\begin{array}{c} B_\lambda^+(y) \\ B_\lambda^-(y) \end{array} \right]$$

with

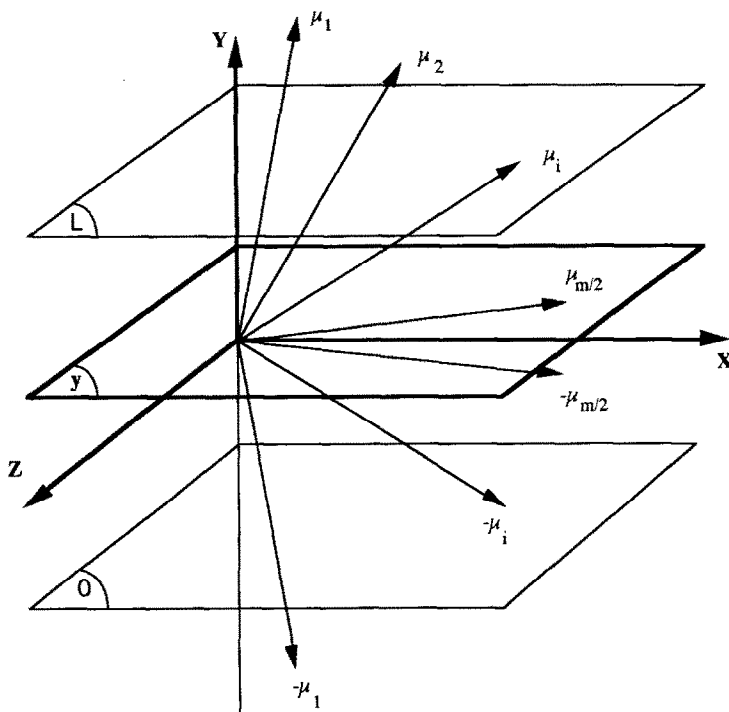


FIG. 1. Directions of discretization.

$$[A_\lambda] = \begin{bmatrix} \alpha & \beta \\ -\beta & -\alpha \end{bmatrix}$$

where α and β are $(m/2) \times (m/2)$ matrices of elements:

$$\alpha_{ij} = \frac{1}{\mu_i} (-\sigma_{ci}(\mu_i)\delta_{ij} + C_{zji})$$

$$\beta_{ij} = \frac{1}{\mu_i} C_{z-ij}$$

$$\text{for } i \text{ and } j = 1, \dots, \frac{m}{2}$$

Two applications will be treated in the following section:

(i) the problem of radiative transfer without internal emission. This is the case encountered in experimental studies using a lock-in amplifier and allowing the determination of the bidirectional reflectance or transmittance. Equation (3) thus simplifies to:

$$\left[\frac{\partial L_\lambda(y)}{\partial y} \right] = [A_\lambda][L_\lambda(y)]; \tag{4}$$

(ii) the problem of combined radiation and conduction. This is a situation often encountered when modelling fibrous materials such as those used in residential or industrial insulations. In this case, an equation of conservation of energy must be added to the radiative transfer equation as will be discussed in Section 5.

3. CALCULATION OF THE RADIATIVE PROPERTIES

In order to determine values for the monochromatic coefficient, the method presented by Lee [17] based on the monochromatic efficiencies (Q_z) as described by Kerker [15] was used here. In the case of fibres stratified in planes parallel to the boundaries, with random azimuthal orientation, one obtains:

$$\sigma_z(\mu) = \frac{1}{2\pi} \int_0^{2\pi} 2rN(r, \omega_r) Q_z d\omega_r \tag{5}$$

where r is the fibre radius and $N(r, \omega_r)$ is the density of fibres of radius r , oriented in the direction ω_r .

The product ' $\sigma_{s\lambda} \cdot P_\lambda$ ' was used to represent the scattering geometry. This is a more convenient approach than calculating a single phase function since this term appears explicitly in the radiative transfer equation. In typical 'two-flux' models, two characteristic factors, one for backscattering and the other for forwardscattering must be found. The scattering cone defined by Kerker is thus divided into two parts which correspond to each hemisphere of propagation. This principle was used here, but instead of considering two single directions, we divided space into m sectors and determined the amount of radiative energy scattered in each sector. We thus considered scattering linked with a given direction of the scattering cone, θ_k , and we determined the direction μ_k that corresponds to θ_k . This led to the elementary quantity:

$$(\sigma_{s,i} P_i)_k(\mu_s \rightarrow \mu) = \frac{1}{2\pi} \int_0^{2\pi} \frac{N(r, \omega_r) \lambda}{\pi^2} I(\theta_k(\mu_s), \phi) d\omega_r \tag{6}$$

where the subscript k indicates that the result is obtained in the θ_k -direction, and $I(\theta_k, \phi)$ is the intensity of the scattered wave as discussed and defined by Kerker [15]. After adding up all the quantities which correspond to the given scattering direction μ_s , bidirectional scattering coefficients were obtained that represented the scattering from one direction μ_s to the direction μ .

Since this method was applied numerically, angle sectors with a given width and centred on specified directions were used in the solution scheme instead of considering only single directions. This method provides the coefficients C_{ij} used in equation (2).

3.1. Numerical results

We studied the case of a medium with a volumetric mass of 10 kg m^{-3} , composed of silica fibres with a diameter of 7 microns oriented in planes parallel to the boundaries. The strongly non-grey behaviour of such a medium has been previously described [8], particularly the Christiansen effect, leading to an extinction decrease at 7.3 microns.

Taking into account the spectral variations of the radiative properties, the influence of the incidence direction at a given wavelength was studied. Values of the different coefficients $\sigma_{a,z}$, $\sigma_{s,z}$ and $\sigma_{e,z}$ are shown in Fig. 2, where it can be seen that there is a decrease of nearly 35% as the incidence angle rises (the minimum is found for an angle of 90° that corresponds to a radiation parallel to the fibres).

Variations of the bidirectional scattering coef-

ficients are given in Fig. 3. The value of the incident polar angle is indicated for each curve, where the part scattered in angular sectors around the different discrete directions is represented. In order to obtain slight variations, we worked on 'scattering sectors' with a width of 2° . Four observations can be readily made:

- (i) the phenomena are strongly anisotropic;
- (ii) there is a scattering peak in the incident direction;
- (iii) a high degree of backscattering was observed (part of the curve between 90 and 180°);
- (iv) a second peak in the specular direction appears as a consequence of the partitioning of the fibres into parallel planes.

Those variations must be taken into account in order to properly model the radiative energy transfer. This type of variation can also be used to explain the limitations of the classical approximations, such as the 'two flux model' which uses only two coefficients to represent the scattering.

In order to test the accuracy of our scattering representation, we compared our results to those of Houston [10], who worked on a medium composed of isotropically oriented glass fibres using a Legendre polynomial expansion to calculate the phase function. Our bidirectional coefficients were calculated under the same conditions, and were normalized by dividing them by the global scattering coefficient $\sigma_{s,z}$. Average values of the scattering phase function in the different angle sectors centres around the discrete directions were thus obtained. The use of a very fine step size then allows the plotting of the phase function profile.

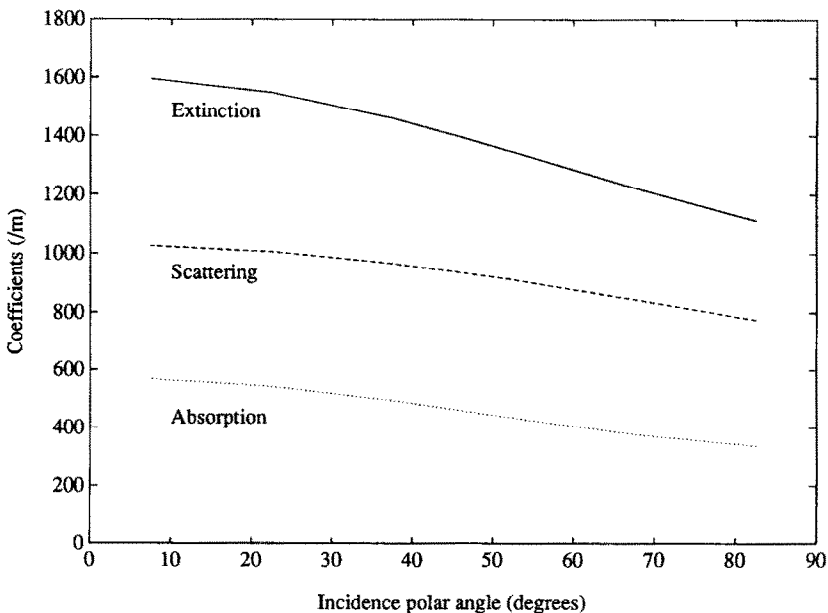


FIG. 2. Variations of the coefficients with the angle of incidence for an incident wavelength of 8.2 microns.

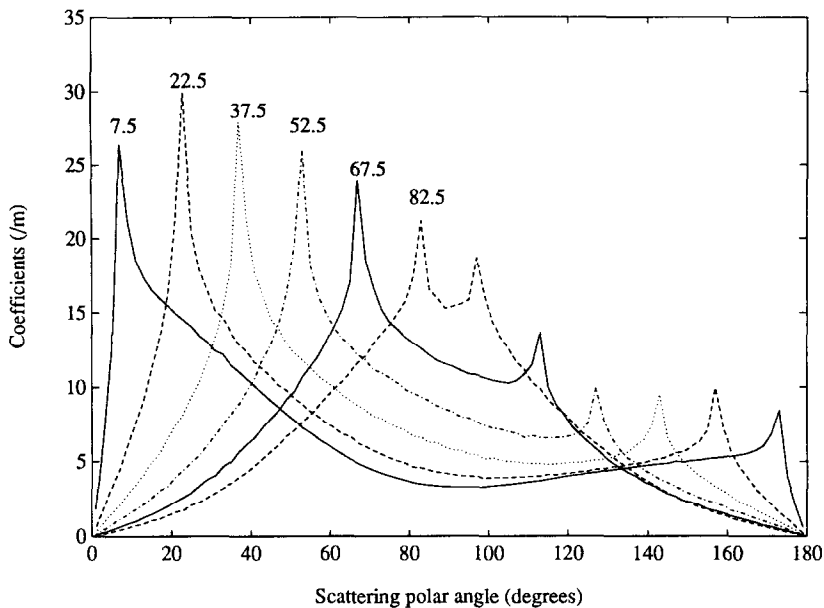


FIG. 3. Scattering representation for radiation of wavelength 20 microns at several incidences (7.5°–22.5°–37.5°–52.5°–67.5°–82.5°). The width of the angular sectors centred around the scattering directions is 2°.

The comparison is presented in Fig. 4, where it appears that our results agree very well with those of Houston for this type of medium. The case of fibres stratified in parallel planes is also shown. The influence of the fibres' orientation becomes clear, especially where increase of backscattering with a peak in the specular direction is seen.

4. HOMOGENEOUS PROBLEM SOLUTION

In order to solve the homogeneous transfer problem, equation (4), which is in fact a system of homogeneous differential equations without a second term, must be resolved. It would appear that a convenient method for solving such a problem is a matrix

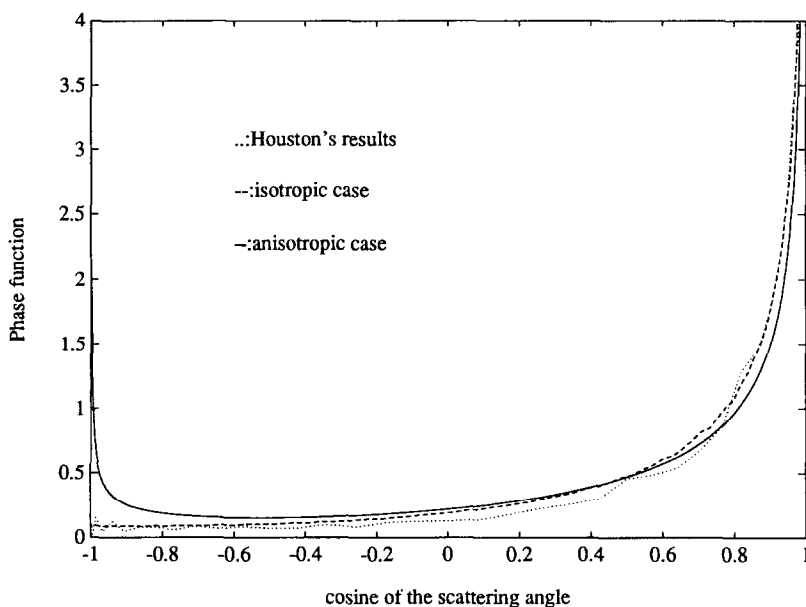


FIG. 4. Comparison of our results with those of Houston at a wavelength of 25 μm and at normal incidence.

exponential method, which suggests a solution in the form :

$$[L_\lambda(y)] = [L_0][\exp(A_\lambda y)]. \tag{7}$$

However, several studies among those reviewed by Flatau and Stephens [12] clearly demonstrate that for the range of optical depth we are concerned with, a direct application of this method would be numerically unstable, thus prohibiting any meaningful interpretation of the results.

A method based on the use of characteristic matrices which take the medium radiative properties into account will therefore be required. These are the transmission and the reflection matrices. The methods for finding such matrices have been reviewed by Flatau and Stephens [12], Waterman [13] and Wiscombe [14]. We chose to use the *Doubling-method*, which beginning with the properties of a very thin layer, allows us to determine the reflective and transmission properties by successive doublings of the medium depth.

Let us define the matrices T_{0y} and R_{0y} as being the transmission and reflection matrices of a medium between the coordinates 0 and y . The problem space is then divided into two hemispheres with intensity distributions of L_λ^+ and L_λ^- . As these are not scalar, but rather vectors quantities, this method is often called the *two-streams* method by analogy with the two-flux method which does not take into account several directions of transfer. Rewriting a radiative transfer equation with these matrices, and invoking the discretization described earlier and the supposition of medium homogeneity; we can write $R_{0y} = R_{y0}$ and $T_{0y} = T_{y0}$, from which we can obtain :

$$\begin{bmatrix} L_\lambda^+(y) \\ L_\lambda^-(y) \end{bmatrix} = \begin{bmatrix} T_{0y}L_\lambda^+(0) + R_{0y}L_\lambda^-(y) \\ T_{0y}L_\lambda^-(y) + R_{0y}L_\lambda^+(0) \end{bmatrix}, \tag{8}$$

Solving the system of equations (8), it becomes possible to determine the intensity distribution at depth y from the intensity at depth 0. For boundary conditions known at two points, which is often the case with the intensities $L_\lambda^-(0)$ and $L_\lambda^-(L)$, we obtain the following system :

$$\begin{bmatrix} L_\lambda^+(y) \\ L_\lambda^-(y) \end{bmatrix} = \begin{bmatrix} T_{yL}L_\lambda^+(0) + R_{yL}L_\lambda^-(y) \\ T_{yL}L_\lambda^-(L) + R_{yL}L_\lambda^+(y) \end{bmatrix} \tag{9}$$

where T_{yL} and R_{yL} are the transmission and the reflection matrices between y and L .

4.1. Case study: modelling of transmittance and reflectance measurements

This type of problem may be solved using system (8) and boundary conditions such as :

$$\begin{cases} L_\lambda^-(0, \mu_i) = L_{0\lambda}[T_0] \\ L_\lambda^+(0, \mu_{i \neq i}) = 0 \end{cases} \tag{10}$$

System (10) expresses an incidence in the direction μ_i : for example the emission of a black body at temperature T_0 .

The problem defined by systems (8) and (10) was solved in terms of $L_\lambda^+(L)$ and $L_\lambda^-(0)$. Twelve discrete polar directions were used in the numerical solution. The spectral variations of the direct transmission are shown in Fig. 5. As expected, certain features such as the transmission peaks at 7.3 and 19.3 microns are observed. These peaks correspond to the wavelength

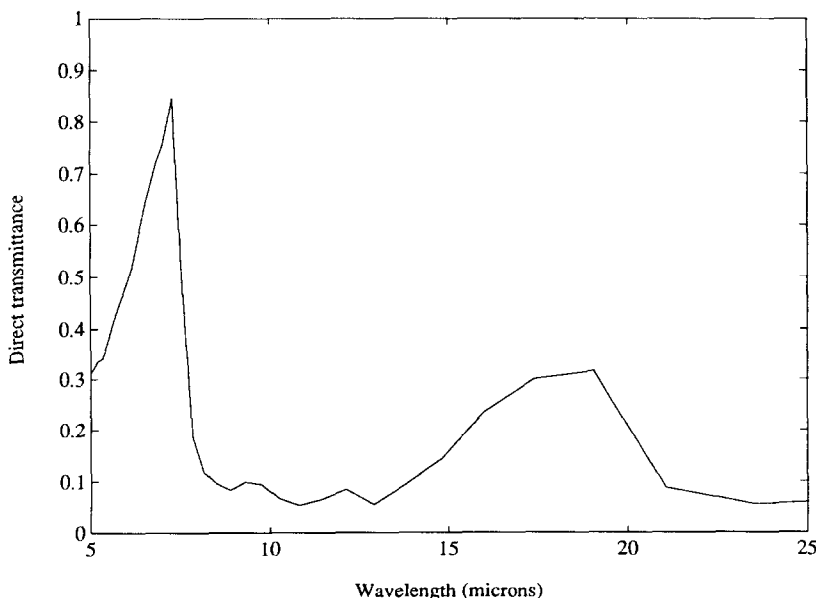


Fig. 5. Normal direct transmittance as a function of wavelength for a medium of a thickness of 2 mm and a volumetric mass of 10 kg m^{-3} .

zone where the radiation extinction falls, as explained through the Christiansen effect.

It is also possible to calculate some hemispherical properties such as those obtained with an integrating sphere. The flux leaving the fibrous medium is given by :

$$F_{\lambda}(L) = 2\pi \int_{\mu=0}^1 L_{\lambda}(\mu, L)\mu \, d\mu \quad (11a)$$

and the incident flux is

$$F_{i\lambda}(0) = 2\pi \int_{\mu_i - \delta\mu_i/2}^{\mu_i + \delta\mu_i/2} L_{\lambda}(\mu, 0)\mu \, d\mu \quad (11b)$$

where L is the depth of the medium, μ_i is the incidence direction and $\delta\mu_i$ is the interval centred around μ_i representing the angular sector of incidence.

The directional-hemispherical transmittance is then given by :

$$\tau_{\lambda}(L) = \frac{F_{\lambda}(L)}{F_{i\lambda}(0)} \quad (12)$$

The theoretical results obtained with this method are shown in Fig. 6. Some experimental measurements have already been made and a more precise experimental validation is in process [19]. An apparatus using a lock-in amplifier, a bolometer working at the temperature of liquid helium, a monochromator, an integrating sphere and an automated rotating system will be used to obtain other results that will be published soon.

5. COMBINED TRANSFERS IN FIBROUS MEDIA

The case of interest in this section is that of combined conduction and radiation. In order to simulate heat transfer through fibrous insulation, the equation of conservation of energy must be satisfied :

$$\text{div}(Q_c + Q_r) = 0; \quad (13)$$

where Q_c is the conduction flux given by :

$$Q_c = -\lambda_c \frac{dT}{dy} \quad (13a)$$

λ_c is the thermal conductivity of the medium and Q_r is the total radiative flux given by :

$$Q_r = \int_{\lambda=0}^{\infty} 2\pi \int_{\mu=-1}^1 L_{\lambda}(y, \mu)\mu \, d\mu \, d\lambda \quad (13b)$$

with $L_{\lambda}(y, \mu)$ obtained from the solution of the radiative problem.

There are several ways to express the conductivity λ_c , for example :

(i) in a linear form as Houston [10] did: $\lambda_c = aT + b$,

(ii) according to another semi-empirical form as Banner [7] did, developing expressions based on experimental data obtained from a guarded hot plates apparatus at the Research Centre of Saint-Gobain.

Note that those expressions may take into account convective phenomena as a corrective term, this gives more generality to our problem.

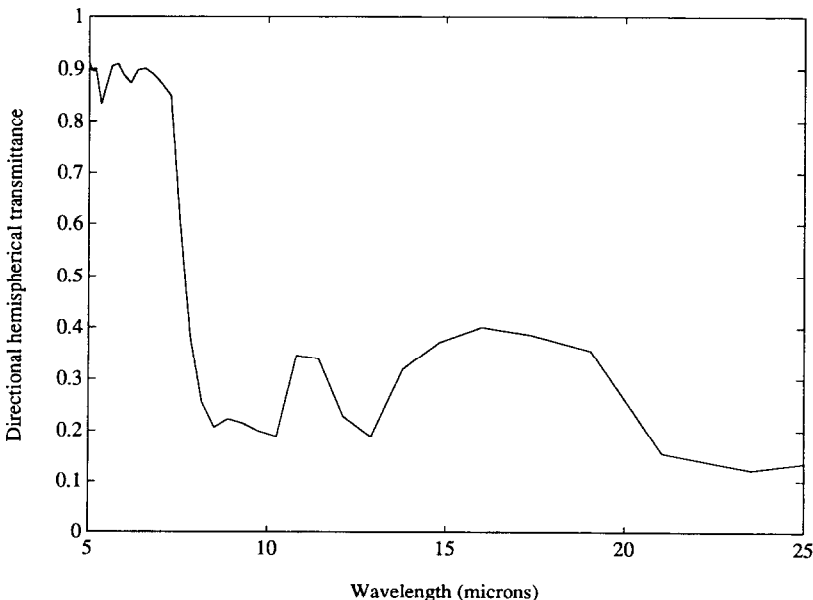


FIG. 6. Directional hemispherical transmittance at normal incidence as a function of wavelength for a medium of a thickness of 2 mm and a volumetric mass of 10 kg m^{-3} .

The coupled nature of the problem is seen through the presence of the temperature distribution in both equations (1) and (13). This leads to a system of two simultaneous equations in two unknowns: T and $L_z(y)$.

5.1. Radiative transfer

This problem has an additional term with respect to that studied in the last section, that being the internal emission of the medium. A look at how the transmission matrices vary with medium depth shows that any influence of external radiation on the medium disappears rapidly. The internal emission term is therefore very important, and has an influence on the intensity distribution far from the material boundaries. For example, in the case of a material composed of silica fibres with a volumic mass of 10 kg m^{-3} , the distance at which the boundaries no longer influence the energy transfer varies as a function of the wavelength, but is on the order of 1 cm. This observation supports Rosseland's approximation, which, however, is not sufficient if we wish to find an exact solution to our problem.

The system of equations to be solved in matrix form is given by equation (3). Suppose that we can write the intensity $L_z(y)$ as the sum of one homogeneous part $L_{h\lambda}(y)$ and a particular part $L_{p\lambda}(y)$, such that $L_{h\lambda}(y)$ is the solution of the homogeneous problem and $L_{p\lambda}(y)$ is the intensity linked to the internal emission. In a classical solution of a non-homogeneous differential equation this would be analogous to seeking an homogeneous and a particular solution.

The homogeneous part satisfies the system of equations (9) in the form:

$$\begin{bmatrix} L_{h\lambda}^+(y) \\ L_{h\lambda}^-(y) \end{bmatrix} = \begin{bmatrix} T_{0y} L_{h\lambda}^+(0) + R_{0y} L_{h\lambda}^-(y) \\ T_{yL} L_{h\lambda}^-(L) + R_{yL} L_{h\lambda}^+(y) \end{bmatrix} \quad (14)$$

The solution to the particular part may be sought in polynomial form:

$$L_{p\lambda}(y) = \sum_{n=0}^N Z_n y^n \quad (15)$$

In order to do this, the term $B_\lambda(y)$ is written as:

$$B_\lambda(y) = \sum_{n=0}^N X_n y^n$$

and the corresponding solutions Z_n are calculated from the transfer equation (see Stamnes [20]).

By identifying the same power coefficients we obtain:

$$\sum_{j=-m_i/2}^{m_i/2} (\sigma_{e\lambda}(\mu_i) \delta_{ij} - C_{ij}) Z_n(\mu_j) = X_n(\mu_i) \quad (16)$$

and

$$\begin{aligned} \sum_{j=-m_i/2}^{m_i/2} (\sigma_{e\lambda}(\mu_i) \delta_{ij} - C_{ij}) Z_n(\mu_j) \\ = X_n(\mu_i) - (n+1)\mu_i Z_{n+1}(\mu_i) \\ (n \text{ from } 1 \text{ to } N-1). \end{aligned}$$

For the applications we are interested in, where the real temperature distribution is nearly linear, only very few terms are needed to exactly represent the internal emission.

To complete the problem the boundary conditions $L_z^+(0)$ and $L_z^-(L)$ are incorporated. In the case of black boundaries we obtain:

$$\begin{aligned} L_z^+(0) &= L_{0z}[T(0)] = L_{h\lambda}^+(0) + Z_0 \\ L_z^-(L) &= L_{0z}[T(L)] = L_{h\lambda}^-(L) + \sum_{n=0}^N Z_n L^n \quad (17) \end{aligned}$$

since $T_{LL} = T_{00} = [I]$ and $R_{LL} = R_{00} = [0]$, where $[I]$ is the identity matrix and $[0]$ a matrix with all elements equal to 0.

The solution of system (17) gives us $L_{h\lambda}^+(0)$ and $L_{h\lambda}^-(L)$, from which $L_{h\lambda}(y)$ and $L_z(y)$ can be calculated at any position y .

5.2. Solution of energy conservation equation

As defined in equation (13b), the spectral radiative flux is integrated over all wavelengths to give the total radiative flux.

In fact, at room temperature and considering the black body emission spectrum we will limit ourselves to the interval $[4 \mu\text{m}, 40 \mu\text{m}]$. To do this we use a thin spectral slice whose mesh becomes finer near the shorter wavelengths.

The solution of equation (13) is then obtained numerically using a finite element method (FEM). The thermal conductivity used is that given by Banner [7]. Values of the temperature, conductive flux and radiative flux are found at every node in the FEM mesh.

Since the problem considered is at room temperature, the radiative portion of the heat transfer flux does not become too important, never exceeding 50% of the total flux. Numerical instabilities do not occur and the requirements of the law of conservation of energy are satisfied, as we will see below in Table 1. However, at higher temperatures a relaxation method would be necessary to obtain the numerical results.

5.3. Results

First we will consider the results concerning the radiative transfer, then look at the characteristics of the total flux. Verification of the grid size indicated that 12 polar steps were sufficient to obtain a correct description of the different phenomena [19]. In fact, comparing our results with other values calculated with 18 polar steps we noted differences never exceeding 0.5%.

(a) Radiative transfer. The results presented in this article were established with a fibre diameter of $7 \mu\text{m}$, which is representative of typical fibre size, and gives a rough idea of the transfer characteristics.

Figure 7 exemplifies typical behaviour of the intensity distribution of a fibrous medium with fibres stratified in planes parallel to the boundaries. The heat flux is found by integrating equation (13b). The spectral

Table 1. Flux variations and temperature distribution within the medium. The volumetric mass is 20 kg m^{-3} , the thickness is 10 cm and the wall temperatures are 293 and 303 K

Thickness (mm)	Heat flux (W m^{-2})	Radiative flux (W m^{-2})	Conductive flux (W m^{-2})	Temperature (K)
0	3.69	0.88	2.81	293.00
5	3.72	0.93	2.79	293.52
10	3.71	0.96	2.75	294.04
15	3.71	0.98	2.73	294.55
20	3.71	0.99	2.72	295.06
25	3.71	1.00	2.71	295.56
30	3.71	1.00	2.71	296.07
35	3.71	1.00	2.71	296.57
40	3.71	1.00	2.71	297.07
45	3.71	1.01	2.70	297.57
50	3.71	1.01	2.70	298.07
55	3.71	1.01	2.70	298.57
60	3.71	1.02	2.69	299.06
65	3.71	1.03	2.68	299.56
70	3.71	1.04	2.67	300.05
75	3.71	1.04	2.67	300.54
80	3.71	1.04	2.67	301.03
85	3.71	1.04	2.67	301.51
90	3.71	1.03	2.68	302.01
95	3.72	1.00	2.72	302.50
100	3.69	0.96	2.73	303.00

radiative flux for two scattering representations, one isotropic case and one anisotropic with respect to planar fibre distribution, is shown in Fig. 8. It is clear that an exact representation of the phase function is needed. (The isotropic case underestimates the real value of the flux by half.) Another parameter which does not appear here is the fibre size. Our calculations

showed that a diameter of approximately $2 \mu\text{m}$ minimizes the heat transfer.

(b) *Combined transfer.* The global heat transfer flux was calculated for several different volumetric masses and temperature gradients. Table 1 presents some typical results obtained with the method presented here.

The accuracy of the model predictions can be seen, especially since the heat flux defined using the law of conservation of energy remains constant. Another interesting result is the nearly linear temperature profile, even though the radiative flux represents approximately 27% of the total flux.

The influence of the volumetric mass is shown in Fig. 9. It is interesting to note that there exists a value for which the heat transfer is minimized. Below this value, the heat flux increases sharply due to an increase in the radiative flux. Above this value, the influence of radiative transfer is negligible but conductive heat transfer contributes to an increase in the total heat flux. This analysis agrees exactly with the behaviour observed thanks to data obtained on a guarded hot plates apparatus [7].

The influence of the coupling of the heat transfer modes can be seen from the temperature distribution. In fact, because of the law of the energy conservation, the temperature profile is non-linear, but this non-linearity is very weak except for very low volumetric masses or for large mean temperatures, in which case the radiative part becomes predominant. This can be seen in Fig. 10 where three profiles calculated with the same cold wall temperature ($T_c = 293 \text{ K}$), but with various hot wall temperatures ($T_h = 303, 333$ and 363 K), have been plotted for a medium with thickness

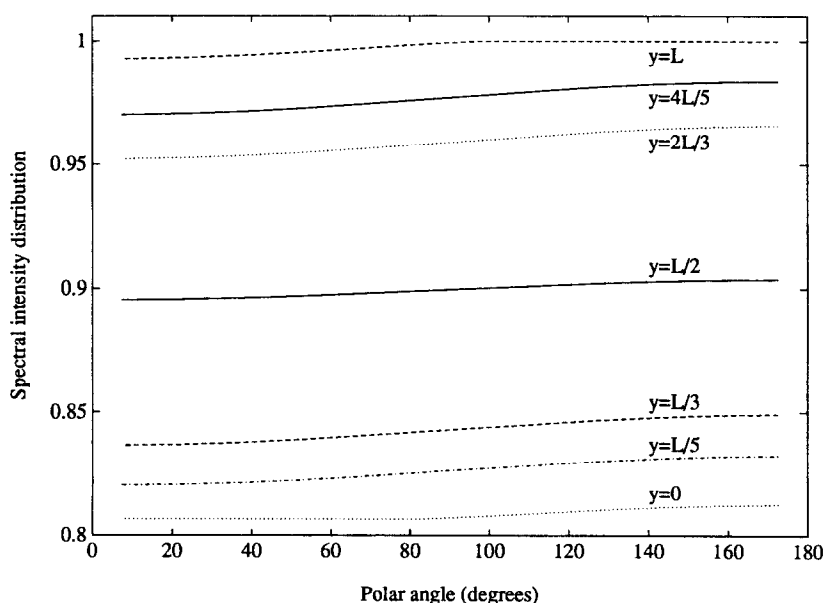


FIG. 7. Spectral intensity distribution for several positions within the medium at wavelength $7.55 \mu\text{m}$. The case of a medium with a volumetric mass of 10 kg m^{-3} , a thickness of 10 cm and with wall temperatures of 293 and 303 K. The results are normalized by $L_{0i}[T(L)]$.

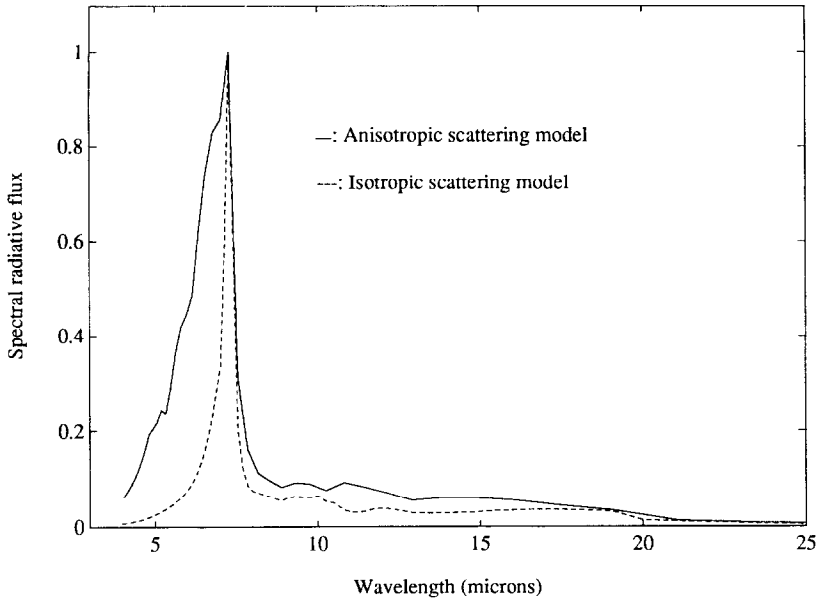


FIG. 8. Spectral radiative flux as a function of wavelength for two scattering representations. The case of a medium with a volumetric mass of 10 kg m^{-3} , a thickness of 10 cm and with wall temperatures of 293 and 303 K. The results are normalized by $\text{Sup}(Q_{\text{ex}})$.

10 cm. As T_b increases, the radiative contribution increases. This leads to a curvature of the temperature distribution. Note that at conditions such as these which are close to room temperature, the deviation of the profiles from linearity is only very slight.

6. CONCLUDING REMARKS

We are able to calculate the radiative properties of fibrous media, and then to accurately model radiative

transfer. The method presented here is based on a spatial discretization technique that allows us to express the radiative transfer equation in matrix form. The solution is then written using the characteristic properties of the medium which are the transmission and the reflection matrices. Since all parameters are taken into account, i.e. the medium morphology, optical properties, spectral variations and anisotropic scattering effects, the model results obtained agree extremely well with available experimental data.

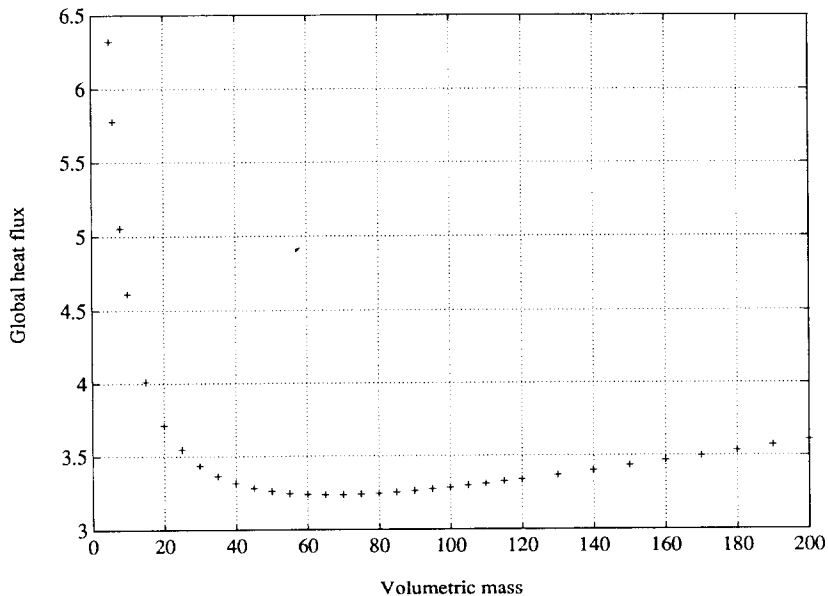


FIG. 9. Global heat flux (W m^{-2}) as a function of medium volumetric mass (kg m^{-3}). The case of a medium with a thickness of 10 cm and with wall temperatures of 293 and 303 K.

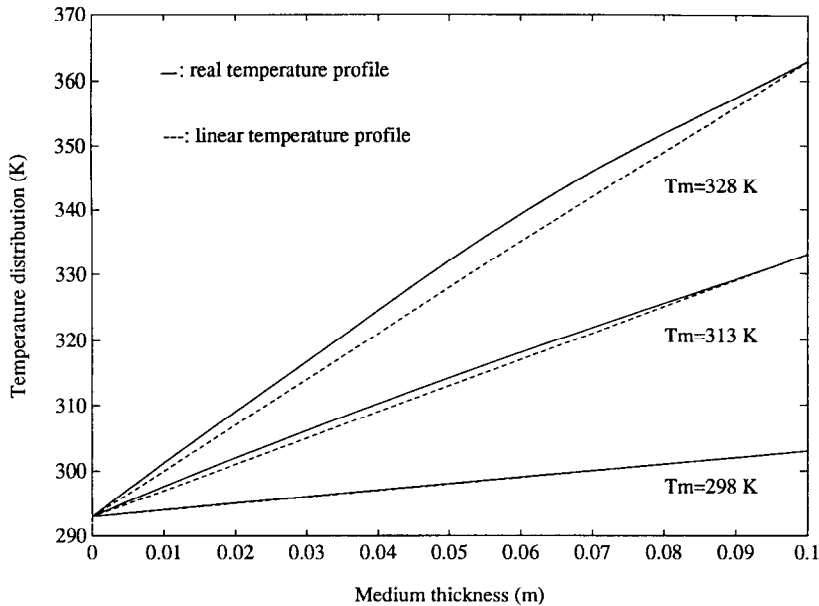


FIG. 10. Temperature distribution within the medium. The volumetric mass is 10 kg m^{-3} and the thickness is 10 cm. The cold wall is at temperature $T_c(0) = 293 \text{ K}$ and the temperature of the hot wall is successively taken at $T_h(L) = 303, 333$ and 363 K . T_m is the mean temperature of the medium.

A more elaborate verification is currently in process.

Note that the method proposed here may be applied to any kind of fibrous media. Moreover, no simplifications such as isotropic scattering or hemispherical isotropy, which are often encountered in other model formulations, have been used.

REFERENCES

1. N. Ozisik, *Radiative Transfer*. Wiley, New York (1973).
2. S. Chandrasekhar, *Radiative Transfer*. Dover, New York (1960).
3. T. W. Tong and C. L. Tien, Radiative heat transfer in fibrous insulation. Part 1: Analytical study, ASME Paper 81-HT-42 (1982).
4. T. W. Tong and C. L. Tien, Radiative heat transfer in fibrous insulation. Part 2: Experimental study, ASME Paper 81-HT-43 (1982).
5. G. Guilbert, Etude des caractéristiques optiques de milieux semi-transparents, Thèse de Doctorat Nancy I, France (1985).
6. G. Guilbert, G. Jeandel, G. Morlot, C. Langlais and S. Klarsfeld, Optical characteristics of semi-transparent porous media, *High Temp. High Press.* **19**, 251–259 (1987).
7. D. Banner, Propriétés radiatives des verres et des fontes de silicates. Modélisation des transferts de chaleur. Thèse de Doctorat, Ecole centrale de Paris, France (1989).
8. G. Jeandel, P. Boulet and G. Morlot, Radiative transfer through a medium of silica fibers oriented in parallel planes, *Int. J. Heat Mass Transfer* **36**, 531–536 (1993).
9. J. A. Roux, A. M. Smith and D. C. Todd, Radiative transfer with anisotropic scattering and arbitrary temperature for plane geometry, *AIAA J.* **13**, 1203–1211 (1975).
10. R. L. Houston, Combined radiation and conduction in a non-gray participating medium that absorbs, emits and anisotropically scatters, Ph.D. Thesis, Ohio State University (1980).
11. R. M. Goody and Y. L. Yung, *Atmospheric Radiation—Theoretical Basis*. Oxford University Press, Oxford (1989).
12. P. L. Flatau and G. L. Stephens, On the fundamental solution of the radiative transfer equation, *J. Geophys. Res.* **93**(D9), 11037–11050 (1988).
13. P. C. Waterman, Matrix exponential description of radiative transfer, *J. Opt. Soc. Am.* **71**(4), 410–422 (1981).
14. W. J. Wiscombe, On initialization, error and flux conservation in the doubling method, *J. Quant. Spectrosc. Radiat. Transfer* **16**, 637–658 (1976).
15. M. Kerker, *The Scattering of Light and Other Electromagnetic Radiation*. Academic Press, New York (1969).
16. A. C. Lind and J. M. Greenberg, Electromagnetic scattering by obliquely oriented cylinders, *J. Appl. Phys.* **37**(8), 3195–3203 (1986).
17. S. C. Lee, Radiation heat transfer model for fibers oriented parallel to diffuse boundaries, *J. Thermophys. Heat Transfer* **2**(4), 303–308 (1988).
18. S. C. Lee, Effect of fiber orientation on thermal radiation in fibrous media, *Int. J. Heat Mass Transfer* **32**, 311–319 (1989).
19. P. Boulet, Etude du transfert par rayonnement à travers les milieux fibreux, Thèse, Nancy I, Décembre (1992).
20. K. Stamnes and R. A. Swanson, A new look at the discrete ordinates method for radiative transfer calculations in anisotropically scattering atmospheres, *J. Atmos. Sci.* **38**, 387–399 (1981).